JOURNAL OF PHYSICS AND CHEMISTRY

CSK SCIENTIFIC PRESS

Review Article
Volume 1 | issue 1

Necessary Revision of Carbon Solid State and Raman Spectroscopy Fundamentals for Comprehensive Mastering of More Performing Advanced Materials Applications

Stephane Neuville

***Corresponding Author:** Stephane Neuville, TCE Independant Consultant15 avenue de la République. F-60330 Le Plessis Belleville Tel 03 4470 0308 Mob.06 4147 1922.

Obtained a degree in physics at Grenoble Polytechnic Institute with Louis Neel in 1970. In 1996 he obtained a PhD at Ecole Polytechnique (X) in Palaiseau France on plasma and thin film technologies.

Submitted: 07 Nov 2023 **Accepted:** 11 Nov 2023 **Published:** 16 Nov 2023

Citation: *Stephane Neuville (2023). Necessary Revision of Carbon Solid State and Raman Spectroscopy Fundamentals for Comprehensive Mastering of More Performing Advanced Materials Applications J of Physics & Chemistry. 1(1), 1-13.*

Abstract

Considering the important potential of more advanced carbon materials for many different domains including mechanical and tribological applications, energy and electrochemical energy storage and conversion and nanotechnologies, their applications used to be hampered by several non-mastered and non-understood effects basing on non-satisfactory established fundamentals of the achievement and characterizing of more performing material structure. They have been very often confronted to conflictual interpretation of Raman spectroscopy and to some non-understood and/or little-known specific phase transformation, especially when these materials correspond to a wide distribution of different homogeneous or more complex polymorph crystalline and amorphous structures with frequently both quite poor and non-reproducible outstanding properties. Thus, needing to be revised to some extent. Much confusing the established definition of carbon Raman D and G bands and when some essential aspects used to be often neglected or incorrectly considered, especially concerning the hypothetical concept of Raman D' and G' peaks specific to atomic disorder, the superimposition of different substructures bands , the internal stress causing shifts of Raman signals which have then to be differently assigned, the locality of some specific phonon breathing modes, the role of atomic disorder on band broadening and last but not least, different sorts of phase transitions with either exothermal or endothermal atomic rearrangements. Last one corresponding to some almost ignored electronic quantum energy activation effects. Clearing comprehensively these aspects is expected to provide the perspectives of well mastered processes for many more performing application domains and particularly the achievement of more efficient production of green hydrogen and cheaper renewable energy, which can then be used for competitive modern transportation systems.

Introduction

Carbon materials appear to have an important potential of improvement of electrochemical energy storage and conversion [1]. Besides more homogeneous crystalline diamond with nearly 100% Csp3 or crystalline graphite a n d gr a p he ne with nearly 100% Csp2, t h e y is generally corresponding to polymorph structures containing different sorts of more or less ordered substructures with a mix of Csp2 and Csp3 (Fig.1). [2]. Carbon material can contain all sorts of carbon structures with isolated Csp2 bonded to other atomic species or with Csp2 clusters and stacks of Csp2 hexagonal cyclic rings forming graphenic particles (more or less curved and distorted single and multi-graphene planes, SWCNT, MWCNT), Nanowires containing a mix of sp2 and sp3 and other more or less amorphous diamond like Csp2/Csp3 substructures (DLC), Rhombohedral diamond microcrystals, H6 and helicoidal diamond, Amorphous (disordered) diamond and tetrahedral Carbon materials (ta-C) we briefly review next. Last ones for which Csp3 rich substructures can be formed with different types of sp3 activation effects (including those with plasma technologies, High energy irradiation, neutralization and noticeable chemical recombination energy release) and some other specific glassy carbon materials which are obtained with thermal reduction of hydrogen rich polymeric carbon materials, without deeper vacuum and plasma technologies, and being themselves either more graphitic or more diamond-like [2-7].

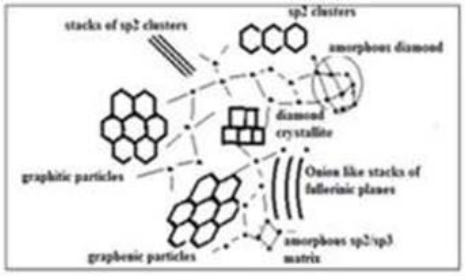

Fig.1 Scheme of composite DLC carbon material

Figure 1: Scheme of composite DLC carbon material.

Whenever considering only main types of structures with some specific combined outstanding properties, they need to be com-

prehensively optimized and mastered for many sorts of new interesting applications of different domains, especially concerning the achievement of more efficient and cheaper green renewable energy production devices and for which it appears that several fundamental features have to be revisited and revised for their well- understood optimized and reproducible implementation [8].

On one hand concerning the possibility to have better detailed and reliable characterization which can be insured with revision of some hazardous aspects of the Raman spectroscopy fundamentals and which request the necessity to revisit some questionable aspects of the associated quantum mechanics, especially concerning its probalistic approach and its locality [9].

*On other hand the necessity to have the different appropriate processes and right implementation equipment's designs with which the different specific carbon material structures with higher thin film properties can be achieved. And for which especially the different mechanisms of the film material growth and different material phase transformation has to be sorted out [3-4, 11-12]. The different sorts of carbon-based materials include more important ones for which many improved elder and new better performing applications can be expected.

A. Carbon Material with High Content of Csp3

90 to 100 GPa hardness Diamond crystalline and polycrystalline (more or less defect free, and crystalline order). Polycrystalline carbon has generally high- rugosity surfaces (if not specifically polished) and an optoelectronic gap in the 4 to 5 eV range which can be tuned with different doping materials. They have generally to be implemented with significant coating thicknesses in accordance with the crystallite sizes (µm range) [4-6].

50 to 70 GPa harder, homogeneous more diamond like ta-C tetrahedral amorphous carbon with tunable optoelectronic gap in the 2-3 eV range with smooth surfaces and possible film thickness in the nm range which can nowadays be produced with reduced internal stress and have relatively high thermal and mechanical stability (~500 up to 700°C) and can be implemented with strong and stable adhesion, insuring combined high optical and optoelectronic and mechanical and tribological properties and which can be tuned with appropriated doping [7,11,12]. They can now present very low wear rates down to factor more than thousand in comparison to other conventional anti-wear DLC materials and with results similar to those of polished multi- crystalline diamond in contrast to results of elder and recent past when they used to be of reduced practical interest, because having high internal stress and poor adhesion strength and stability or becoming almost graphitic degraded to much less performing DLC after thermal annealing and however, for which modern solutions are now available [3-17] .

10 to 30 GPa so called Diamond-Like coatings (DLC) including a-C:H (hydrogenated harder carbon materials with reduced thermal stability (<300°C).

[3, 13-14]. Better properties (higher hardness, higher thermal stability etc.) can be achieved with High Power Impulse Sputtering for which the temperature of the substrate/growing film coating system is kept rather low (avoiding thus significant thermal graphitic degradation, meanwhile higher ionization and activation of the particles which are impinging on the growing film is provided. Thus, contributing to more diamond like DLC, whenever with lower Csp3 than with other processes achieving harder ta-C [7, 11-13].

Graphitic Materials with High Csp2 Content

Graphenic materials with ordered juxtaposed hexagonal cyclic rings content. They present excellent electric conducting properties and low energy optoelectronic gap which can be tuned with appropriate doping [4,12]. They are used for optoelectronic and mechanical nanotechnology applications generally associated to other types of thin film materials and incorporated in metal alloys for their strengthening. To be noted, that their adhesion to neighbor materials can be provided via doping and internal edge of vacancies and voids, considering that graphene smooth surfaces, have quite passivated solid- state properties. Should be aware, that these can be subject to sp3 phase transformation, with some newly rediscovered effects to be particularly considered [4].

Amorphous graphite (GAC) and Diamond Like Carbon with low Csp3 content. They are generally obtained with thermal evaporation, when under specific process time and temperature their recrystallization is avoided. Concerning the Csp2 rich DLC, they are obtained with thermal annealing and graphitic degradation of more diamond-like DLC and diamond, when the Csp3 phase transformation conditions (electronic quantum activation) are not enough fulfilled [2-4].

Glassy Carbon (porous disordered stacks of mainly graphemic materials). Specificity of these materials is that they can be produced without refined vacuum and plasma technologies. Despite their porosity, they have good proton diffusion barrier properties, which can be combined to antierosion and anticorrosion [3, 17]. However, they can appear with different electric conductivity and different hardness and what used to be not understood up to recent past, and hampering their use for practical applications, when the quality and reproducibility of the results could not be secured. These problems are suggested to be essentially due to some non-understood Raman spectroscopic analogy with highly diamond like materials for which close neighbor Raman peaks (band) corresponding either to Csp3 or to Csp2 cluster edges not sufficiently differentiated [4, 14-17], although having different properties, and which are depending from some phase transformations not always be known or correctly identified and for which different sorts of glassy carbon must be distinguished.

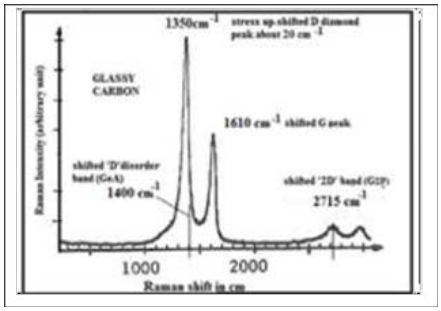

Figure 2: Diamond Like Glassy Carbon ~25 Cm-1 Stress Upshift Shown on G Peak [18]. Apparent Raman similitude with polycrystalline diamond Fig.6. However, differentiated with stress-shifts (20 cm-1 downshift for fig.6 and 25 cm-1 upshift for Fig.2 with different peak assignments [18].

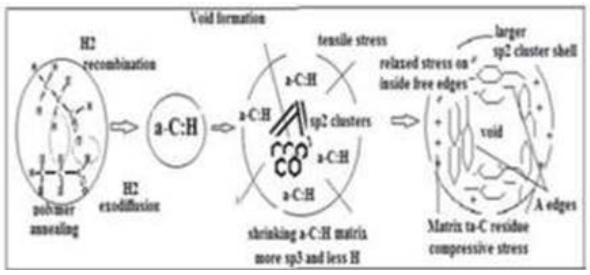

Figure 3: Scheme of S P 2 Glassy Carbon Formation. Voids Grow with H2 Exodiffusion Causing Tensile Stress [12]. Glassy carbon can have higher hardness with the formation of sp3 by electronic quantum energy activation (H2 chemical energy release), if not degraded with longer high temperature annealing (1000K,30mn) [18-19].

Harder more dielectric diamond-like glassy carbon (with significant Csp3 content) with high anticorrosion and anti-abrasive properties, for which its existence was often much ignored up to now – contrary to the graphenic glassy carbon [18-19]. This is obtained when their process temperature and process time are significantly lower than for graphenic Glassy Carbon (for instance~700°C during about one hour, instead of 1400°C during two hours), a n d which is transforming a polymeric material into Csp3 rich material with H2 chemical recombination energy release activation.

Less hard graphenic glassy carbon with more Csp2 content, and no hydrogen left which is achieved with same sort of process than for precedingly described diamond-like one, but with higher temperature and longer high temperature annealing processes which is transforming polymeric material into hydrogen free graphenic composite material [16-18], considering that Diamond, ta-C and DLC materials are subject to graphitic degradation with longer annealing time and higher temperature [2, 4,10-19].

Carbon Film Material Characterizing

Factual Characterizing.

This is corresponding to usual means with which carbon thin film materials are characterized on their technical properties (mechanical, electric, optical and optoelectronic and thermal properties etc.). However, for which refined interpretation and well understood mastering of reproducibility request more careful consideration for corresponding theoretic fundamentals of solid-state physics we revisit next. Recall, that wear rates are proportional to f.E/H when the adhesion is strong enough (no film delamination) and both intrinsic material and adhesion are thermally stable enough (with f the coefficient of friction, E the elasticity and H the hardness) [20].

Hardness. It is equivalent to the density of cohesion energy (number of interlinked chemical bond x energy of bonds) [2,21]. It can be determined with different indentation techniques for which must be considered the radius of the indentation tip apex, considering that with a larger tip radius than the indentation depth the hardness measurement value will be overestimated [22].

Stress. It is a very important material feature which can deeply affect the adhesion and the robustness of thin film materials and which must be evaluated before being reduced with some appropriate optimized process conditions. Must be i d e n t i f i e d different internal and external stress w h i c h can be added to each-others [2].

The best stress reduction has to be obtained with the optimization of some combined process conditions. The internal stress (which is film thickness dependent) can be measured with the deformation amplitude of a disc [23]. Its optimization can only be achieved if the relation between the process conditions and the achieved material properties can be established and for which the revision of corresponding fundamentals will help to sort them out.

It must be distinguished different sorts of compressive and the tensile intrinsic stress, which can be associated independently to materials with different properties. The total stress of a thin films corresponds to the addition of: a) the integration of the intrinsic stress over the coating thickness, (including thermal stress), b) the interface stress depending on atomic pseudo lattice mismatch at the film/substrate interface, and c) the external stress (local external pressure). Addition of them can decisively affect the adhesion strength. However, this depends also, on the actual density of the interfacing atoms binding energies and which can be affected by the stress. Therefore, also, depending on interlayer contamination and surface passivation of the substrate. To be noted the very decisive and helpful aspect, that stress can be determined with some up- or downshift of some characteristic spectroscopic Raman peaks correctly identified, we present in §III.

Adhesion. This can be measured with some scratch test, which contrary to some other methods, is providing an adhesion strength which is not affected by some associated deformation energy [24]. Some confusion between Adhesion energy and adhesion strength must here be avoided. Conversely to elder popular belief, the adhesion strength is notproportional to the intrinsic adhesion energy (addition of all atomic interfacing binding energies per unit area) but corresponds to the energy of delamination which includes the energy of the newly created material surfaces with some atomic rearrangements. It can be determined

with some scratch test (conversely for instance to the pull test, for which the delamination energy includes an important deformation energy) [24].

Local atomic packing density. It is influencing cohesion, porosity and diffusion properties and adhesion strength, considering that interface atomic disorder and interface atomic pseudo lattice mismatch induce some Interface stress. Last ones can be determined at least qualitatively for instance, with transmission electron microscopy.

Surface rugosity to be observed with scanning electron microscopy. Combined with hardness and interfacial affinity to counter-facing material, it can significantly enhance the coefficient of friction and the wear rates with some local delamination of hard material.

Contamination and surface passivation. They can deeply affect the adhesion strength and its stability, into addition to the stress and which can be characterized with surface science analytical means. To be noted that surface contamination and passivation can also result from the process vacuum base pressure with residual hydrocarbon and water vapor which can be adsorbed on the substrate surface or which can be incorporated in the growing film material. Recall that at 10-4 Pascal vacuum, the condensation of residual species can cover a surface up to one atomic/molecular layer per second when the substrate surface material and/or the growing film material is chemically reactive and/or with high surface adsorbtion properties for the impinging species (especially at lower temperature) [2-4].

Optical properties. Theses, includes transparency, reflexion, diffraction, refraction properties. They are quite interdependent and can be used to verify the specificity of a material, whenever never with univoqual parameters. For instance, soft polymeric material can have similar optical transparency than very hard ta-C, but with different reflecting properties and dif f erent diffraction coefficient. To be noted, that longer more intense photon irradiation can induce some material structure modification. On one hand, they can generate heat which degrades carbon material to more graphitic ones. On other hand, especially with harder irradiation (X rays and harder UV etc.) they can be transformed to more sp3 rich materials with some electronic quantum energy activation) [2-4].

Atomic Binding Structures in Materials

Sp2 and sp3. Conversely to widespread belief, this is not the only criteria to be considered for the achievement of harder diamond and diamond-like carbon material or specific graphemic materials. For instance, frozen CH4 has 100% Csp3 and nothing in common with diamond, because of weak interlinking H bonds in its bulk. Also, to be considered that amorphous graphite (GAC) with 100% Csp2 and high concentration of vacancies and voids, has little in common with much denser and ordered crystalline graphite and other ordered graphene and carbon nanotubes. Some other material characteristics have to be associated, such as specific general structure and local substructures and distribution of interatomic bonds and binding energy. It used to be nevertheless considered as a first classification frame for carbon materials considering the huge material property differences between Graphite and Diamond [2-3].

Considering that for the determination of the sp3/sp2 ratio some characterizing devices appear to be quite complex (NMR), it used to be determined, with some other apparent simpler methods with the ID/IG ratio of corresponding Carbon Raman and with XPS photoelectron spectroscopy [4-9]. We will explain in next paragraphs why theses appear hazardous and questionable. However, the sp3/sp2 ratio can be quite accurately determined with XPS Auger spectroscopy (electronic energy transition involving three different levels) specific to sp2 and sp3 configuration and less depending from surrounding bonds (verified with synchrotron Xray near edge spectroscopy [25,26].

Structure phase transformation and thermal stability. Considering the difference between endothermal or exothermal chemical reactions [21]. Last one corresponds to a specific transformation towards a lower global internal energy and to its groundstate. Meanwhile endothermal reactions correspond to an atomic rearrangement towards a metastable structure with higher internal energy. It has been shown for instance, that a graphitic material can be transformed towards diamond and diamond-like materials, with some electronic quantum energy activation and which can be observed with different sorts of higher activation energy input (including combination of heat and pressure which modify the interatomic binding energy) [10].

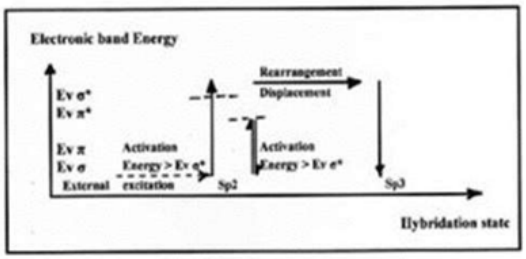

Figure 4: Scheme of Quantum Electronic Activation of Sp3 Atomic Rearrangement (> 1 eV)

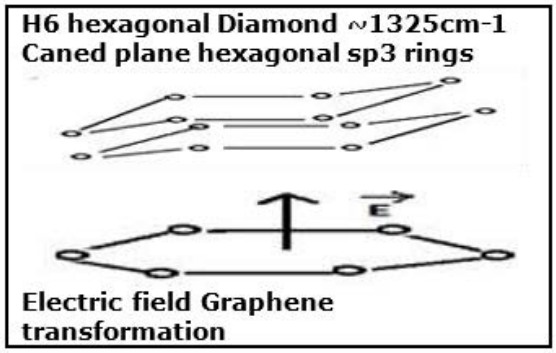

Figure 5: Transformation of Stacks of Csp2 Hexagonal Rings of Graphene into Buckled Plane H6 (Hexagonal Diamond) with an Electric Field [2].

We show with Fig.4 and Fig.5 an example with the endothermal transformation of graphene planes into H6 diamond, much different from thermal activation with energy (T=1200K ~0.1eV

<< than the optoelectronic gap of potentially achievable diamond like (~1 eV) and diamond structures (~5 eV).

During the thermal annealing of carbon materials, heat with phonon energies 0.01 up to 0.1eV range, will favorize the phase transformation towards its groundstate (graphite) with an exothermal process, considering that no sufficient local activation energy input can activate valence band electrons up to higher conduction bands for some newly rearranged other structures with higher internal energy. Denser, harder DLC, ta-C and diamond are degraded to more graphitic materials at temperature > 200°C up to 800°C, depending on their actual atomic packing density and amount of atomic disorder, vacancies and dangling bonds [4, 8-9]. These phase transitions are subject to several conditions [10].

- Compatibility of electron activation with energy levels of the final state.
- Stochiometric and steric conditions. Spatial distribution of stronger bonds and impurities of atomic range size can hamper the atomic rearrangement.
- Competition between electron quantum activation and thermal graphitization which depends on the respective power of each transformation competitors and on their respective activation /decay kinetics.

The formation of sp2 hexagonal cyclic ring clusters is achievable with thermal energy at T > 250°C (> ~0.05 eV). Meanwhile the formation of sp3 clusters is requesting some activation energies > ~ 1-5 eV range. To be noted that diamond microcrystals can be formed with the electronic activation energy released with the recombination of H to H2 (~5eV) or with N to N2 (~12eV) depending on their respective concentration of dissociated species and diffusion kinetics [9, 27]. This is what happens for instance with some highly activated process plasma containing many dissociated Nitrogen and N+ ions which can recombine on a growing CNx film material surface, contrary to low density plasma where essentially non dissociated Nitrogen and N2+ ions are present. An effect, which could not be understood and expected with usual established solid-state fundamentals. Thus, why these have to be revised and what we discuss in next § III and IV.

Ordered crystalline and disordered more or less amorphous structures. This can be identified with neutrons and X-rays diffraction and different low and high energy electron beam/ material surface interactions, we will not describe in details here. However, to be observed that those are more difficult to be implemented when the material is a mix of micro- and nano-size structures and for which other spectroscopic techniques have to be used in association with adequate spatial resolution and analysis of interatomic binding energies.

Interatomic Binding Characteristics

Ir Spectroscopy

This provides information on interatomic phonon vibration which are depending on atomic weight, interatomic distance and binding energy specific to interatomic binding configuration (such as OH, CH, CO, CC etc.). To be considered that, the interatomic binding energy of carbonated molecules is also depending on the hybridization state of the carbon atom. However, which is providing reduced information on the general global and local solid-state material structure and its properties [28].

Xps Spectroscopy

The energy of photo-electrons extracted from internal atomic energy shells, is subject to the modification of the valence band energy level with the additive effects of all its surrounding chemical bonds. The corresponding spectroscopic chemical shift is univocal when the material is homogeneous and contains a unique type of bonds. Considering that a determined hybridization state is influencing it's surrounding binding energies, XPS was thought being able to determine the sp2/sp3 ratio.

However, a hybridization state cannot always be clearly identified when a defined hybridization is bonded to several others and which is introducing some chemical shift band broadening. Csp3-Csp3 bonds will be different from Csp3-Csp2 and from Csp2-Csp2 and Csp2XYZ different from Csp2 X'Y'Z' etc. (X, Y, Z the atomic species bonded to a same sp2 carbon atom). However, an XPS spectrum will include also, some Auger electron signals which are less influenced by the chemical bonds and more specific for its hybridization state [25].

Raman Spectroscopy

It can provide detailed information about a carbon material structure considering that the corresponding spectra are resulting from the interaction of photons with a material structure where it will first excite some electron which is either activating some phonon (bond vibration) specific to the material structure or which will receive the energy of the specific phonon [29]. However, those, which cannot always be coherently understood with the use of current quantum mechanical solid-state fundamentals which did not consider the locality of the corresponding effects. Emphasizing that Raman spectroscopy is providing information on the solid-state structure of clusters of atoms where specific interatomic phonon vibration exists. Therefore, which need to be revisited in more details and we discuss next [8-9].

Confusion in Current Carbon Raman Spectroscopy

Apparent Raman Spectra Similitude of Different Carbon Materials

Raman spectra apparent similitude is causing a lot of confusion for the correct determination of the structure of carbon materials and their expected properties to be used for different applications. We present next some quite illustrative examples, which can be sorted out, in considering some revisited and refined analysis with a detailed larger number of differentiated solid-state aspects than originally popularized.

Comparison of Some Polycrystalline Diamond and Some Glassy Carbon

Raman spectra of non-perfect polycrystalline diamond with some diamond like glassy carbon (with Fig.6 and Fig.2) look quite similar, when not considering their respective stress-shift and not considering some possible atomic rearrangements of graphitic glassy carbon towards more diamond like one.

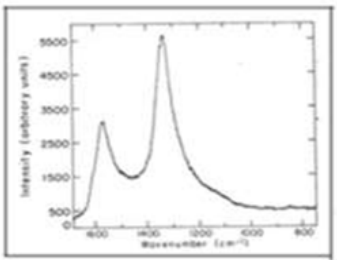

Figure 6: Polycrystalline Diamond [30]. Diamond crystallites embedded in sp2/sp3 matrix achieved with 7,4% HC and 22% C13 isotopes. Tensile stress downshift ~20 cm-1 of Ddiamond crystalline peak ~1310cm-1 on "D disorder" band base line. G peak ~1560cm- 1. Diamond Shoulder ~ 1150cm-1.

Glassy carbon w a s k n o w n to be generally quite graphemic with very low sp3 content, in contrast to some hereby presented one (Fig.2) [18] which is here particularly diamond-like, what can be seen with some refined analysis of the D peak which can either correspond to a diamond structure (nominal frequency at~1330 cm-1) or to some graphene A-edge vibration mode (nominal frequency at~1350 cm-1) and which can be clearly identified with high enough spectral resolution because of the rather high sharpness of the different D and G peaks.

Comparison of Amorphous Graphite with Amorphous Very Hard Ta-C

Another illustrative example is given with the comparison of very hard amorphous carbon (ta-C) (Fig.7) with quite soft amorphous graphite resulting from some low energy or ions irradiation of glassy carbon [Fig.8] [15,31]. The apparent similar shape of the Raman spectra, might erroneously suggest the same type of material.

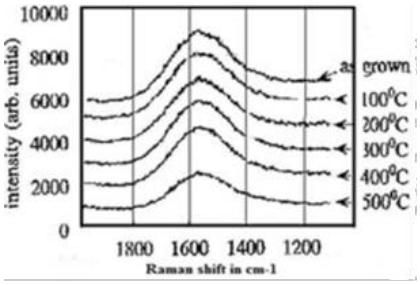

Figure 7: Stress Differentiated Apparent Similitude For 500°C Annealed and as Grown Ta-C (60/80GPa, ~80%sp3). Compressive stress-shift ~100 cm-1. Max~1570 cm-1 for stress- upshifted DG band (nominal ~1460cm-1) on as grown ta-C. Reduction of Csp3-Csp2 bonds (DG band). Few sp3 clusters ~1430cm-1 and few disordered hexagonal cyclic Csp2 rings band ~1680 cm-1. After s t r e s s annealing, no stress-shifted band for disordered Csp2clusters ~1580cm-1 [15].

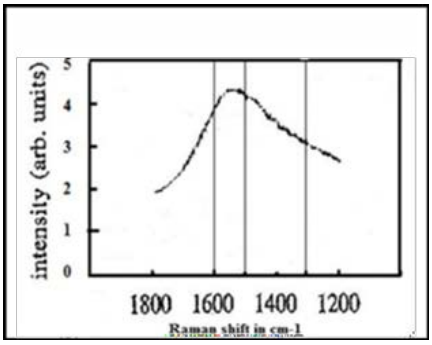

Figure 8: Amorphous Low-Energy ion Irradiated Glassy-Carbon [31]. Low Compressive-stress. Ion Neutralization Energy Release, Can Form Sp3 (non-crystallin ~1300 cm-1 band). No specific G peak = > No Ordered Hexagonal Sp2 Ring Structures ~1580cm-1. Gband Max ~1560 Cm-1 For Disordered C5/C7sp2-Ring. Shoulder~1450cm-1 Suggests some few Csp2-Csp3 Clusters.

However, a major point which used to be almost neglected during the past is that those spectra can be much different, when each of them has a different internal stress with corresponding stress-shift of the Raman spectra and therefore, with different material structures. With the shown Fig.7 of mentioned work [15], the temperature annealing of ta-C materials can gradually reduce their internal stress, and causing at same time gradually their transformation to their groundstate (graphitization) and which can favorize their graphitic recrystallization. It is then expected that the original band corresponding to harder amorphous carbon (ta-C) will be reduced, but with differently shifted Raman frequencies, depending on actually achieved stress reduction. Much harder ta-C and diamond species, are known to present higher thermal stability and for which the stress will be differently reduced according to annealing temperature and to different annealing time. A quite confusing situation with effects which used to be not always clearly understood we suggest to be comprehensively sorted out with following.

The broad Raman band of ta-C corresponds to a Raman disordered diamond band and which is containing a band (~1460cm-1) corresponding to some specific substructure with mixed Csp3 and Csp2 (we designate DG) which is ~100 cm-1 compressive stress-shifted. It is to be further-on considered that because of it highly disordered aspect (close to amorphous diamond) and with better distributed Csp2 and Csp3, only a reduced amount of Csp3 clusters will be maintained.

Thus, explaining why only a band of reduced intensity at 1430cm-1 is observed (corresponding to a nominally non-shifted disordered diamond band ~1330cm-1). The temperature annealing reduces the stress and the intensity of this band (lower content of Csp3-Csp2 bonds) and the newly obtained band is then characteristic for a more graphitic disordered Csp2 material. However, for which only reduced amount of ordered cyclic hexagonal Csp2 rings will exist explaining why no intense band ~ 1580cm-1 appears (Fig.7).

Stress Reduction with Thermal Annealing and Atomic Rearrangements

The wish to combine both the stress reduction (mainly for the achievement of more stable and stronger adhesion) with the higher properties of some pristine more diamond like materials which were not yet thermally annealed, was for long time up to recent past, supposed impossible to be satisfied. Harder more diamond like amorphous ta-c materials combining superior optical, opto- electronical, electric/dielectric, mechanical and chemical inertness properties have been considered to have always redhibitory high stress, and which unfortunately could not be reduced without significant graphitic degradation, loosing thus, the benefit of more performing diamond properties [13-14].

However, this redhibitory graphitization during a thermal annealing can be avoided with some additional electronic quantum energy activation, considering that with this activation graphitic materials can be converted into more diamond like and diamond materials (discussed in § II). It must then be correctly sorted out that temperature annealing reduces the stress and intensity of this band and the newly obtained band is then characteristic for a more graphitic disordered Csp2 material. However, for which only reduced amount of cyclic hexagonal Csp2 rings will exist explaining why no intense band ~ 1580cm-1 appears (Fig.8).

Stress Reduction with Thermal Annealing and Atomic Rearrangements

The wish to combine both the stress reduction (mainly for the achievement of more stable and stronger adhesion) with the higher properties of some pristine materials which were not yet thermally annealed, was up to recent past supposed impossible to be satisfied. Harder more diamond like amorphous ta- c materials combining superior optical, opto-electronical, electric/dielectric, mechanical and chemical inertness properties are usually presenting redhibitory high stress, and which unfortunately could not be reduced without significant graphitic degradation, loosing thus, the benefit of more performing diamond properties [13-14]. However, this graphitic degrading can be avoided with some additional electronic quantum energy activation, considering that graphitic materials can be converted into more diamond like and diamond materials with this effect (discussed in §II). It must then for this purpose be correctly and completely sorted out both, the corresponding revisited Raman spectroscopy for clearer characterizing of the material at each process step to be adjusted and optimized, and the material phase transformation fundamentals as well.

Atomic Disorder Raman Band Broadening and Band Superimposition

Recall that a well-ordered crystalline structure will only show narrow peaks corresponding to mono frequency phonons. Meanwhile a Raman band is always corresponding to some disordered structure with broader distribution of interatomic distances and phonon frequencies (Fig.9 and Fig.10) [9, 32].

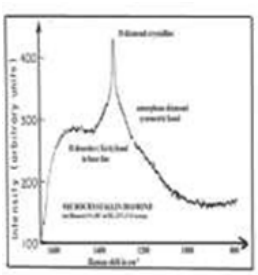

Figure 10: Ordered Crystalline D Diamond Peak, Compared to Disordered and Diamond Corresponding to Symmetric Broader D Diamond Band At ~1330cm-1 [33]. (Different from The Graphene Aedge Vibration Mode At ~ 1350cm-1 (A K Vibration Mode) And Questioning the Existence of a So-Called Ddisorder Peak.

This, other erroneously almost neglected effect brings all the more confusion, when Raman peaks are transformed to Raman bands corresponding to other substructures than those corresponding to the D and G bands and when in addition those can be overlapping with higher disorder band broadening (Fig.11) [34].

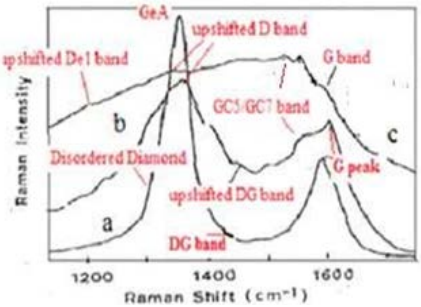

Figure 11: Raman Spectroscopy Analysis of Glassy Carbon Before and After Irradiation with 125kev N+ Ions. Gradual up-shift up to 30cm-1, before downshift with higher ion dose producing amorphizing and heat exodiffusion of recombined N2 molecules, lower atomic packing density and tensile stress downshift. Some DG bands can be observed corresponding either to Csp2-Csp3clusters [34].

However, last but not least which is providing worse confusion when in contradiction to the precedingly mentioned disorder band broadening effects, some identified D and D' peaks have been assigned to the atomic disorder and erroneously called D disorder peaks and which used to appear at neighbor similar Raman shift frequencies than for the D diamond and G graphite peaks [40]. To be discussed next in proposing a newly revised concept.

Revision of Some Carbon Material Fundamentals

Criticism of Established Fundamentals

Necessity to Better Know what is Affecting the Carbon Material Properties

With established fundamentals, it was up to recent past not understood for instance why Graphene and Glassy Carbon properties do not always have the expected better electric conducting properties, or reproducible adhesion strength and stability, and what is causing the so- c a l le d "Graphen Rippling" effect. Also,

why more performing ta-C film material could not be used in practice because of its high internal stress and not known how to reduce it without graphitization, up to now (although now possible to day) [3-4,11,18-19].

It is known that the electronic properties of graphene and graphenic carbon are depending on the asymmetry of their structure with either metallic or semiconducting properties and on their edge configuration, independently from additional doping [41]. However, it must be either pointed out he role of point defects, vacancies and voids (which are not easily characterized), on their possibility to be filled with some dopants and which can affect their elasticity for instance with substitutional Nitrogen atoms and able to create strong film/substrate interfacing bonds, considering the surface passivation of graphene and the very low interplane binding energy of defect free graphite in the 0.1 eV range (graphene can easily be produced by spallation of graphite) [2].

Also, which sort of effect might be converting graphene in so-called "graphane" which appears is in fact quite unlike, considering the higher affinity of hydrogen for another H (~5eV) than for carbon (~4eV) and the high binding energy of C-C bonds (~7eV). It is actually corresponding to the phase transformation of graphene into some buckled H6 diamond Fig. 4 and Fig.5 [9].

Hazardous Determination of Sp3/Sp2 with Raman Spectroscopy Considering that the hybridization state of carbon is clearly making the difference between graphite and diamond, it was concluded that all other types of carbon material would have been possible to be characterized with their sp3/sp2 ratio and to be determined with the respective intensity of distinct D and G peaks of Diamond and Graphite and corresponding to sp2 and sp3 carbon hybridization.

- Quite defect free larger diamond mono crystal (with only Csp3) is showing a single Raman D peak (Diamond peak ~1330cm-1).
- Quite defect free larger graphite crystal (only Csp2 hexagonal cyclic ring cluster structure) and for which edge effects can be neglected) has an intense unique G Graphite peak ~1580cm-1.
- Atomic disorder is creating a distribution of interatomic distances, with which the energies will be distributed accordingly with the broadening of the Raman peak to a larger band [9-32]. For such unique cases, the respective integration of the D and G peaks (or bands) (ID and IG) are actually corresponding to some Csp3 and Csp2 concentration.

However, this is an early-stage classification for carbon materials supposed to give account for their specific properties, which appears quite non-appropriate, considering that most carbon materials are more complex and contain substructures with distributed Csp2 -Csp3 bonds and with Raman shifts different from the original D and G peaks. The D band will therefore, not necessarily contain only Csp3 and a G band not always only Csp2. Notwithstanding the point that, some very hard amorphous tetrahedral carbon materials are only presenting a broad apparent more or less shifted G band, whenever almost containing Csp3. Thus, explaining why the ID/IG ratio classification will be generally meaningless.

Locality of the Raman Effect and Local Atomic Rearrangement Micro Raman studies show clearly some local atomic rearrangement of graphene plane edges, with ZZ-edges being transformed into symmetric A- edges after annealing [35-36]. This is a local effect, which cannot be predicted and described with established usual non-localized probalistic approach of quantum mechanical calculus and which will not be shown with macroscopic Raman spectroscopy showing only non-localized structure modification [37].

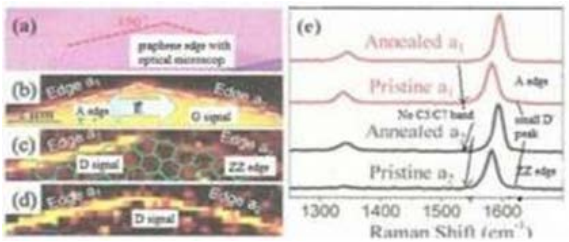

Figure 12: Study of ZZ edge Transformation into A-edge with thermal annealing and micro- Raman of pristine graphene with ~20 cm-1 tensile down-shift. Stress-shift is reduced with thermal annealing ~300°C and recrystallization. So-called D'disorder peak ~1620 cm-1 is reduced on both type of A- and ZZ- edges. Ddisorder peak corresponds in fact to an ordered local A-edge and D'disorder peak to Csp2-Csp2 dangling bonds [36-37].

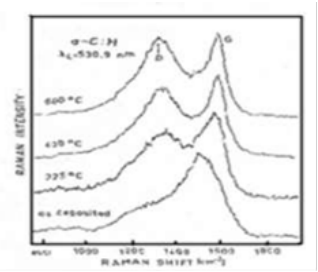

Figure 13: Annealing of a-C: H. Macro-Raman tensile stress resulting from recombined H2 exodiffusion, and growth of disordered Csp3 substructures (broad peak). stress reduction with non-shifted sharp G peak. Phase transformation locality cannot here be considered [38].

On a material plane resulting from the cut of a bulk graphite tansverse to its graphene planes (Fig.14 and Fig.15), a double peak (band) appears: a) a Raman band shoulder at ~1330cm-1 is indicating a diamond like substructure resulting from the mechanical cutting energy input activation which is transforming locally on the separated graphene surfaces, graphene material parts into diamond-like carbon [38]. The broader band ~1330cm-1 indicates that this corresponding diamond-like substructure is quite disordered. b) A quite sharp so- called Ddisorder non-stress shifted peak at ~1350 cm-1 within the non-stressed ordered graphite bulk material (no stress shift is observed on a quite sharp G peak ~1580cm-1) [37]. The same Raman spectrum of graphene plane resulting from a cut of graphite is indicating in

addition a so-called D' disorder peak at ~1620cm-1 and which is also identified with IR spectroscopy [39]. Altogether, suggesting that the often used "Ddisorder" designation during the past up to now is much confusing and almost non-appropriate.

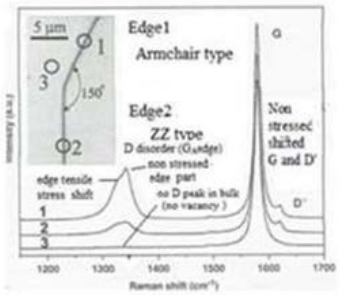

Figure 14: Raman spectra of cut exfoliated graphene [38]. showing no atomic disorder (sharp G peak) and no stress-shifts. Diamond band ~1330cm-1 for graphene rearranged to Csp3 structure with cutting energy input activation, graphene Aedge vibration ~1350cm-1 and Csp2-Csp2 dangling bonds (erroneously called Ddisorder and D'disorder peaks).

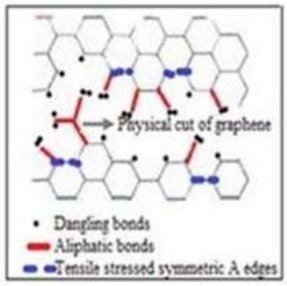

Figure 15: Scheme of cut graphene producing edge Csp2-Csp2 dangling bonds ~1620cm-1 erroneously assigned to so-called D' disorder peak. Dangling Csp2-Csp2 have same signal frequency than with IR [39]. 2D' for double dangling bonds ~ 3240cm-1 [9, 41].

Erroneous Concept of So-Called Disordered Carbon Raman Peaks

It is known that disordered carbon can be formed with the irradiation of more or less crystalline ordered carbon materials with an Argon ion beam [35]. It can be observed, that two main new specific quite narrow bands appear (Fig.14 Fig.16) the so-called "Ddisorder" peak (at nominal ~1350 cm-1) and the so- called D 'disorder peak (at nominal ~1620cm-1) if no stress-shift is modifying the Raman frequency). The observed new peaks after irradiation have then to be assigned to some new atomic structures which are not necessarily correlated to each- others and therefore, not the expression of disorder (as shown on Fig.17 [42].

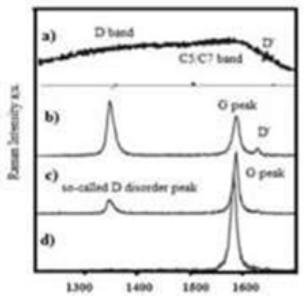

Figure 16: Raman spectra of Ar+ ion irradiated graphene showing that so-called D and D'disorder peak cannot correspond to atomic disorder (broad bands and never a narrow peaks). However, Disorder appears with higher ion doses which are producing important band broadening and band overlapping for all substructure Raman signals [40].

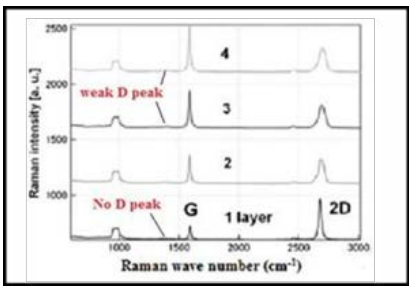

Figure 17: ~10cm-1 upshifted Raman spectra of annealed graphene [42]. No "Ddisorder" (G Aedge) and no D' peak,". Sharp G and 2D peaks: (Ordered recrystallized materials). 2D is an overtone of the weak D diamond peak and not linked to a graphene A edge vibration mode and which can be assigned to graphene rippling (transformation into H6 diamond).

With preceding shown edge effects (Fig.14 and Fig.15 in § IV.1.3) with which the Ddisorder a n d D ' disorder peaks appear respectively corresponding to a) Symmetric graphene A-edge phonon vibration mode and b) some adjacent Csp2- Csp2 dangling bonds [4, 39] and considering some annealing results of modified non-stressed graphene materials (no stress-shift of univoqual identified G peak) well-ordered graphenic structures (sharp G peak) (Fig.17) where nevertheless.

some weak residual sp3 substructures can be identified with a diamond structure overtone mode (2D). Fig.18 and Fig.19 we discuss next § IV.2.

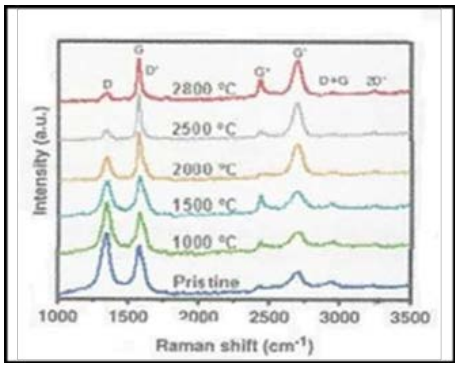

Figure 18: Raman spectra of graphene ribbon annealed at different temperatures [43]. With different phonon vibration modes "Ddisorder" (in fact G Aedge), G, G'(in fact 2D ~2700cm-1), (D+G) ~ 2950cm-1, G'' (iTOLA ~1950cm-1), G* (~2400cm-1), D'(~1620cm-1) and 2D'(3250cm-1) for single and double aliphatic Csp2-Csp2.

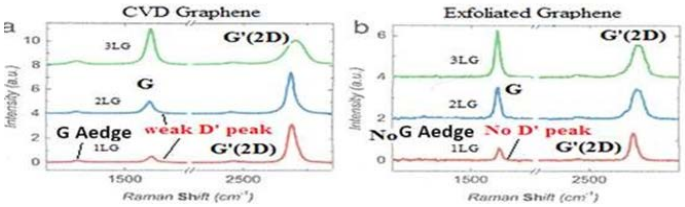

Figure 19: Process dependent so-called Ddisorder (G Aedge) peak (~1350cm-1) in CVD graphene or with exfoliated graphite. Broader G and G'(2D) band caused by some disorder of 3 layers CVD graphene, but with weak G Aedge (~1350cm-1) and weak side band (dangling Csp2-Csp2 ~1620cm-1). Meanwhile sharper G and G' (2D) peaks and no "D disorder" peak for exfoliated graphene (from graphite elaborated with high temperature processing which reduces disorder and stress. [44].

Anomalies of The Raman Quantum Physics Reciprocal Space Description

The Raman effect used to be described with a quantum mechanical scheme in the reciprocal-space with a double resonance mechanism.

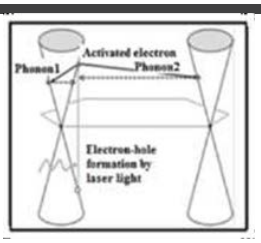

Figure 20: Schematic abstract representation of Raman double resonance in the reciprocal space not giving account for phonon backscattering, locality and conservation law of energy, only the conservation of impulse [38].

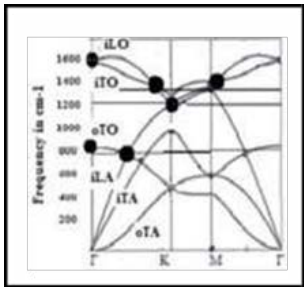

Figure 21: Phonon dispersion curve of graphene. G Raman ~ 1580cm-1 is a double degeneracence of in plane phonon mode on the Γ point. Raman shift ~1350cm-1 is an in- plane vibration of graphene A edge on K point [45].

It shows how a photon is reemitted after some interaction sequence of photon/electron, electron/phonon, phonon backscattering, phonon/ electron and electron deactivation. However, this schematic representation appears to be hazardous, considering that the conservation of energy is not respected (only the conservation of the impulse) and without considering the necessary locality with which local Edge vibration effects can be induced (described in former IV.1.3.).

Revisited Raman Effect Description

Coupling of different modes (same frequency) and stationary wavesWe show with Fig.22 some main graphene vibration modes where a couplin between different modes can be evidenced.

K phonon mode ~ 1350cm-1 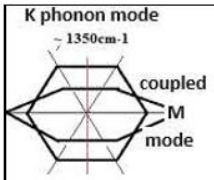 K and M vibration mode coupling on graphene A edge (same frequency).	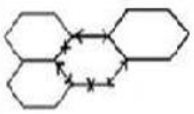 G Raman signal ~ 1580 cm-1 on Γ point. Stationary in plane coupled K and M phonon modes	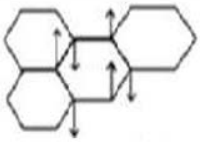 Ternary symmetry 3ω resonance. Stationary mode out-of-plane coupled longitudinal vibration ~ 850cm-1	mode out of plane with coupled longitunal vibration ~800cm-1 on K/2point Binary symmetry 2ω resonance. Stationary mode out of plane coupled longitunal vibration ~800cm-1

Figure 22: Main Graphene Coupled Vibration Modes

Raman Effect Described with Coupled Double Resonance (CDR)

Considering the coupling of activated electron/hole pairs and taking into account the differences between phonon/electron and much higher photon/electron scattering time and the differences between slow decay of activated electron and fast decay of phonon activated holes, it is possible to represent the double resonance Raman effect with a sequence which is respecting both the conservation law of energy and impulse, and which can take into account some locality of the effect we represent with Fig.21. [9].

With equal phonon scattering statistic of electron no Raman effect can result. Meanwhile the contrary when taking into account the phonon scattering statistic of hole and considering some electron/hole coupling, because the phonon/electron scattering time is much lower than the photon/electron scattering time and considering some quasi-immediate decay of phonon activated holes in comparison to the relatively low decay of activated electron.

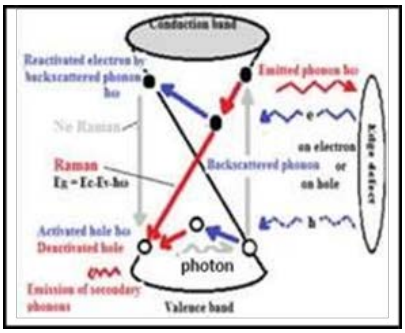

Figure 23: Scheme for a Coupled Phonon Double Resonance Scattering (CDR)with backscattered phonon on same originally activated electron/hole system with conservation of energy and impulse [9].

With the same phonon and electron locality, some 0° angle backscattered emitted phonon on some defects will interact with the originally same activated electron/hole system, thus, explaining why a Raman effect with a coupled double resonance can exist.

Raman Effect Conditions on Local Lattice Edge

Location of Cdr Raman Effect

With the previously described CDR, it appears that a Raman signal can be produced on some symmetric edge structure where a 0° angle backscattering of emitted phonon can exist and considering that the corresponding wave-vector has the same orientation in the reel space and in the reciprocal space. This is observed for instance on graphene symmetric Aedge at nominal ~1350cm-1 (when not affected by any stress shift) and which has nothing to do with any specific peaks supposed to be linked to disorder and we call a G A edge peak.

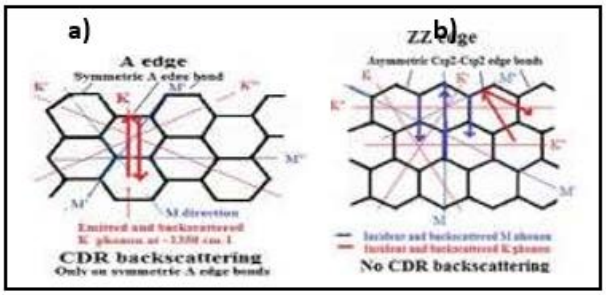

Figure 24: a) One phonon CDR 0° angle backscattering on graphene symmetric Aedges, CDR scattering with in-plane Kphonon ~1350cm-1 (wave-vector ∓ to Aedge).
b) No CDR Raman 0° backscattering on asymmetric graphene Aedge and on ZZ edges.

Noteworthy is, that this Raman signal ~1350cm-1 appears in the vicinity of the D diamond peak (~1330cm-1) and will be quite often incorporated in a broader D band although not linked to any Csp3 content, but only to some s p e c i f i c Csp2 substructure. Thus, which used to bring confusion on the significance of a D band which is not only depending on sp3 content and which integration (ID) can be therefore, meaningless. When a graphenic material is showing a quite intense sharp so-called "D peak" then must be cleared if it is corresponding to the transformation of a graphenic structure to a diamond structure (which is then likely corresponding to the Graphene Rippling effect which is forming some caned H6 diamond nominal ~ 1320/1325 cm-1[9], or if it corresponds to some well-ordered Aedes atomic rearrangement consecutive to some graphitic recrystallization for instance, and which has to be sorted out with other spectroscopic means (like Auger or RMN or IR etc.) and looking if some specific superimpositions of bands can be considered.

Addition of Phonons of Different Raman Signals

Some peaks appearing on a Carbon Raman spectrum can correspond to a double frequency overtone and which can help sorting out more or less overlapping bands, considering that better spectroscopic resolution can be achieved when doubling the spectroscopic scale. Different phonons with different wave vector orientation can interfere with some stationary vibration modes on a same location and produce a Raman CDR effect when all relative conditions are fulfilled.

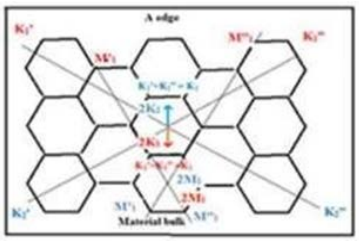

Figure 25: Two Phonon Double Frequency Cdr Raman Scattering ~2700 Cm-1 In the Bulk of Graphene Material with.
*Symmetric K' and K" modes forming a '2K' mode.
*Symmetric M' and M" modes forming a '2M'mode.
No CDR scattering with K+M mode
On internal A-edges of voids CDR Raman effects can be there produced with addition of another symmetric phonon e.g. (G +G Aedge), meanwhile some other will not e.g. (G+Ddiamond).

This includes the 0° angle backscattering which can be achieved when two symmetric phonon waves are interfering on a stationary wave on same location what we show with Fig.25.

Definition of a Revised Carbon Raman Spectroscopic Nomenclatures

With preceding acquired and in order avoid some confusions and to facilitate the better differentiate carbon substructure assignments and the corresponding properties, we propose a new nomenclature (Table 1)

Table 1: Refined Carbon Raman Nomenclature

Raman Frequency cm-1	Band Peak	Structure	Bonding Energy (eV) Non stressed structure
1330	D diamond peak	Ordered cubic	Csp3-Csp3 ~ 7.02
1325	DH	Ordered sp3 hexagonal	Csp3-Csp3 ~ 7.025
1200/1400	D band	Amorphous diamond ta-C	Csp3-Csp3~ 7.02 +/- 0.01
1150	Dedge	Diamond boundaries	Aliphatic Csp3-Csp3
1580	G peak	Plane hexagonal Csp2 ring	Csp2-Csp2 ~ 7.03
~1500-1700	G band	GAC amorphous graphite Superimposed bands	Csp2-Csp2 ~7.03 +/-0.01
~1350	G Aedge	Csp2 hexagonal ring cluster symmetric Aedge	In plane Raman active with plane polarized laser light
~ 1540	GC5	C5 sp2 odd rings	
~ 1550	GC7	C7 sp2 odd rings	
~ 1470	DG	Csp3 cluster- Csp2	Modified Diamond peak
~ 1620	Gsp2	Dangling Csp2-Csp2	Same phonon frequencyIR
~ 1560	GD	Csp2 cluster-Csp3	Modified G peak
~150	RBMG- G+	CNT radius breathing CNT in plane transversal	Distorted Csp2-Csp2 By plane curvature
~1570		CNT in plane longitudinal	
~1590			
~2680	G2P	Two phonon scattering	Addition of K and M modein graphene.
~2700	G3ω	3rd harmonic overtone out of plane optical mode in graphene ~900cm-1	

Conclusions

With some revision of carbon material Raman fundamentals and after considering all together a) some eventual stress shift (compressive or tensile) which can either be mechanically measured or determined with the Raman shift of some re markable unequal Raman peaks, b) some eventual possible atomic rearrangements with transformation of graphitic material to more diamond- like and diamond materials with endothermal electronic quantum energy activation with energetic photons or with different release of neutralization and chemical recombination energy, c) The exothermal thermal degradation of carbon materials towards their graphite ground state , d) the correct assignment of observed bands and peaks considering preceding aspects and e) the adhesion strength and stability in some stacks of thin films or on some substrates, it will be possible to avoid confusion on their reel solid state structure configuration and about their corresponding properties and with which will be expected the achievement of reproducible optimized well understood

and mastered implementation of carbon thin film materials with higher combined properties for many different identified applications [2-4,8,12].

References

1. S Neuville (2018) Materials Today Proceedings AEM 2016 Differentiated Carbon Material for Energy Storage and Conversion 5: 13837-13845.
2. S. Neuville, A Matthews (2007) Thin Solid Films 515: 6619-6653
3. J. Vetter (2014) Surf Coat Tech 257: 213-240.
4. S. Neuville (2019) MDPI Micromachines. Special Issue of Carbon-based Electronic Devices 10: 539-581
5. P.K. Bachmann, W van Enckevort (1992) Diamond Relat Mat 1: 1021-1034.
6. I M Buckley Golder, A T Collins (1992) Diamond Relat Mat 1: 1083-1101.
7. D R McKenzie, E Muller, E Kraftchinskaia, D Segal, D J H Cockaigne (1991) Thin Solid Film 206: 198-203
8. S Neuville (2016) Mat Day Proceeding AEM 5: 13816-13826.
9. S. Neuville (2014) (Book) Carbon Structure Analysis with Differentiated Raman Spectroscopy. Lambert Academic publishing Eds ISBN978-3-659-48909-9.
10. S Neuville (2011) Surf Coat Tech 206: 703-706.
11. S Weissmantel, S Reisse, D Roost (2004) Surf Coat Tech 189: 268- 273.
12. S Neuville (2004) QScience Connect 1.
13. G A Amaratunga, V S Veerasamy, C A Davies, W I Milne, D R McKenzie, et al. (1993) Non-Cryst Solids 1666: 1119-1122.
14. J Robertson (1994) Diamond Rel Mat 6: 361-368.
15. A Anders J (2017) of Applied Physics 121: 1101.
16. D Janas, K K Kozial (2004) Nanoscale 6: 3037.
17. X Zang, Q Zhou, J Chang, Y Liu, L Lin (2015) Microelectron Eng 132: 192-206.
18. A R. Badzian, P K Bachmann, T Hartnett, T Badzian, R Messier (1987) European Materials Research Society Symposia Proceedings XVII Amorphous hydrogenated carbon films. Les Editions de Physique. Strasbourg 63-77.
19. O J A Schueller, S T Brittain, C Marzolin, G M Whitesides (1997) Chem Mater 9: 1399-1406.
20. S Neuvillen (2009) JPJ Solids Struct 3: 33-42.
21. D F Schriever, A T Atkins (1999) Inorganic Chemistry New York. Oxford University Press 197.
22. A Fischer Cripps (2006) Surf Coat Tech 200: 4153-4165.
23. G G Stoney (1909) Proc R Soc A Lon 82: 172.
24. P J Burnett, D S Rickerby (2002) Thin Solid Films 154: 1987403-1987416.
25. C Scheuerlein, M. Taborelli, N Hilleret, A Brown, M Baker (2002) ApplSurfSci 202: 57-67.
26. L Fayette, B Marcus, M. Mermoux, G Tourillon, K Laffon, et al (1998) Le Normand. Phys Rev B 57: 14123-14132.
27. D G Liu, J P Tu, C F Hong, C D Gu, S X Mao (2010) Surf Coat Tech 205: 152.
28. E Fuente, J A Menéndez, M A Díez, D Suárez, M A Montes Morán (2003) J. Phys Chem B 107: 6350-6359.
29. Z Li, L Deng, I A Kinloch, R J Young (2023) Raman spectroscopy of carbon materials and their composites. Progress in Materials Science 135: 101089.
30. K M McNamara, K K Gleason, G J Vestyck, J E Butler (1990) Diam Rel Mat Vol.1(1992) 1145 31) S. Prawer, F. Ninio, I. Blanchonette, J. App.Phys 68: 2361.
31. S Prawer, F Ninio, I Blanchonette (1990) App.Phys 68: 2361.
32. Y Pauleau, C Donnet, A Erdemir (2008) Tribology of DLC Springer New York 102.
33. P V Huong, B Marcus, M Mermoux, D K Veirs, G Rozenblatt (1992) Diam Rel Mat 1: 8696.
34. M. Iwaki, K. Takahashi, A Sekiguchi (1990) J. Mat Res 5: 2562-2566.
35. Y You, Z Yu, Z Shen (2008) App Phys Lett 93:163112.
36. Y N Xu, D Zhan, L Liu, H Suo, Z H Ni et al (2011) ACS Nano 5: 142.
37. J Wagner, M Ramsteiner, C Wild, P Koidl, P. Koidl, et al. (1987) EMRS Meeting XVII, Proceedings by Les Editions de la Physique (Eds) 351.
38. L G Cançado, M A Pimenta, B R Neves, M S Dantas, A Jorio (2004) Phys Rev Lett 93: 247401.
39. B Dischler, P Koidl, P Oelhafen (1987) EMRS Meeting Proceedings by, Les Editions de la Physique 189.
40. M S Dresselhaus, A Jorio, A G Souza Filho, R Saito (2010) Phil Trans R. Soc 368: 5355.
41. K A Ritter, J W Lyding (2009) Nat Mater 8: 235-242.
42. E Watanabe, A Conwill, D Tsuya, Y Koide (2012) Diamond Rel Mat 24: 171.
43. J Campos Delgado, Y Kim, T Hayashi, A Morelos Gomez, M Hofmann (2009) Chem. Phys. Lett 469: 1-3.
44. A Reina, X Jia, J Ho, D Nezich, H Son, et al. (2009) Nanoletters 9: 30-35.
45. M Lazzeri, C Attaccalite, L Wirtz, F Mauri, (2008) Phys Rev B Vol 7: 081406.